



Letter

Preparation and electrochemical studies of $\text{Li}_3\text{V}_2(\text{PO}_4)_3/\text{Cu}$ composite cathode material for lithium ion batteriesT. Jiang^a, Y.J. Wei^b, W.C. Pan^a, Z. Li^a, X. Ming^a, G. Chen^b, C.Z. Wang^{b,*}^a College of Materials Science and Engineering, Jilin University, Changchun 130012, China^b College of Physics and State Key Laboratory of Superhard Materials, Jilin University, 1788 Linyuan Road, Changchun 130012, China

ARTICLE INFO

Article history:

Received 8 July 2009

Received in revised form 25 August 2009

Accepted 27 August 2009

Available online 1 September 2009

Keywords:

Lithium ion battery

Cathode material

Composite material

Electronic conductivity

Electrochemical kinetics

ABSTRACT

$\text{Li}_3\text{V}_2(\text{PO}_4)_3/\text{Cu}$ composite cathode material was prepared via sol–gel method by adding of 1.8 wt% Cu powder into the precursor solution. The structural and physical properties, as well as the electrochemical performance of the material were compared with those of Cu-free $\text{Li}_3\text{V}_2(\text{PO}_4)_3$. X-ray diffraction showed that Cu did not enter the crystal structure of $\text{Li}_3\text{V}_2(\text{PO}_4)_3$. The $\text{Li}_3\text{V}_2(\text{PO}_4)_3/\text{Cu}$ composite material had a higher electronic conductivity comparing with that of Cu-free $\text{Li}_3\text{V}_2(\text{PO}_4)_3$. Electrochemical impedance spectroscopy showed that the adding of Cu decreased the charge transfer resistance of the electrode. In addition, the lithium diffusion coefficient was prominently enhanced from 1.3×10^{-9} to $2.8 \times 10^{-8} \text{ cm}^2 \text{ s}^{-1}$. Based on these advantages, the $\text{Li}_3\text{V}_2(\text{PO}_4)_3/\text{Cu}$ composite material exhibited much better cycling performance than the Cu-free $\text{Li}_3\text{V}_2(\text{PO}_4)_3$.

© 2009 Elsevier B.V. All rights reserved.

1. Introduction

Polyanion materials such as LiFePO_4 [1–3], LiCoPO_4 [4], LiMnPO_4 [5] and $\text{Li}_3\text{V}_2(\text{PO}_4)_3$ [6–9] have been intensively studied as cathode materials for lithium ion batteries. The framework of these polyanion materials is constructed by a rigid $[\text{PO}_4]^{3-}$ network, which helps to stabilize the crystal structure of the materials. The oxygen atoms are fixed in the $[\text{PO}_4]^{3-}$ structure. This limits the likelihood of oxygen liberation, which leads to good thermal stability. On the other hand, incorporation of the $[\text{PO}_4]^{3-}$ groups also raises the charge–discharge potentials of the materials by the “inductive effect” [10].

Among these polyanion materials, $\text{Li}_3\text{V}_2(\text{PO}_4)_3$ has the largest theoretical capacity, which is 197 mAh g^{-1} based on three Li^+ ions are extracted from the material lattice. $\text{Li}_3\text{V}_2(\text{PO}_4)_3$ exists in two forms: a rhombohedra phase and a monoclinic phase. The latter has a close packing structure and shows better electrochemical properties. Monoclinic $\text{Li}_3\text{V}_2(\text{PO}_4)_3$ has a NASICON-type structure which is different from that of olivine LiFePO_4 . This NASICON-type structure has the ability to facilitate faster Li^+ diffusion. However, as most of polyanion materials, the separated $[\text{VO}_6]$ octahedral in $\text{Li}_3\text{V}_2(\text{PO}_4)_3$ reduces the electronic conductivity of the material, which is an intrinsic drawback to its electrochemical performance. In order to increase the electronic conductivity of $\text{Li}_3\text{V}_2(\text{PO}_4)_3$, it is a

common practice to prepare carbon coated materials [11,12]. Recently, some other researches showed that the electronic conductivity of $\text{Li}_3\text{V}_2(\text{PO}_4)_3$ could be improved by cation or anion substitution [13–15].

Another simple approach to enhance the electronic conductivity of cathode materials is mixing the precursor with some conductive metal powders. For instance, Croce et al., increased the specific capacity of LiFePO_4 from 110 to 140 mAh g^{-1} by adding of 1.0 wt% metal powder (Ag or Cu) into the precursor solution [16]. This approach was also successfully adapted to some other cathode materials such as LiCoO_2 [17], LiMn_2O_4 [18] and $\text{LiNi}_{1/3}\text{Co}_{1/3}\text{Mn}_{1/3}\text{O}_2$ [19]. However, up to now this approach has never been proposed for improving the electrochemical performance of $\text{Li}_3\text{V}_2(\text{PO}_4)_3$. Herein, in this work, we prepared $\text{Li}_3\text{V}_2(\text{PO}_4)_3/\text{Cu}$ composite cathode material using sol–gel method. The electrochemical performance of the material was compared with that of Cu-free $\text{Li}_3\text{V}_2(\text{PO}_4)_3$. Based on this, the effects of Cu additive on the electrochemical performance of $\text{Li}_3\text{V}_2(\text{PO}_4)_3$ was studied and discussed.

2. Experimental

For the preparation of $\text{Li}_3\text{V}_2(\text{PO}_4)_3/\text{Cu}$ (hereby named as LVP-Cu) composite material, a NH_4VO_3 and LiH_2PO_4 mixture was firstly added into a glucose solution. The molar ratio of Li:V:P:glucose in the solution was adjusted as 3:2:3:0.3. Then 1.8 wt% of Cu powder was dispersed in the solution and a gel was obtained by heating and stirring the solution at 80°C . This solution was then dried at 120°C to get a precursor. The precursor was pressed into a pellet and pre-treated at 320°C for 4 h in nitrogen flow until the decomposition reaction was completed. The resultant mixture was grounded and pressed into a pellet again, followed by heat treating at

* Corresponding author. Tel.: +86 431 85155126; fax: +86 431 85155126.
E-mail address: wcz@jlu.edu.cn (C.Z. Wang).

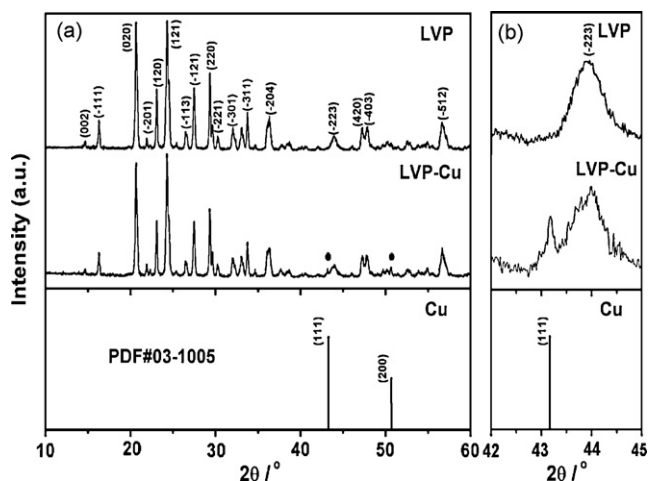


Fig. 1. (a and b) X-ray diffraction patterns of the LVP and LVP-Cu samples, together with that of Cu metal (PDF#03-1005) as a reference.

750 °C for 5 h in nitrogen flow. The preparation of Cu-free $\text{Li}_3\text{V}_2(\text{PO}_4)_3$ (named as LVP) followed the same procedure as described above but without adding of copper powder.

X-ray diffraction was performed on a Rigaku AXS D8 diffractometer with Cu $K\alpha$ radiation. The diffraction data were recorded in the 2θ range of 10–60° with a scan rate of 3° min^{-1} . The cell parameters were calculated by the Celref3.0 Package. The morphological features of the materials were studied by scanning electron microscope (JSM-6700F). The existence of copper in the composite was confirmed by energy dispersive spectrometer (EX-84055BE). The electronic conductivity of the materials was measured on a Keithley2400 Source Meter by the van der Pauw method.

Electrochemical experiment was carried out using a two-electrode coin battery cell. A metallic lithium foil served as the anode electrode. The cathode electrode was composed of a mixture of $\text{Li}_3\text{V}_2(\text{PO}_4)_3$ active material (75 wt%), carbon black conductive additive (10 wt%) and poly-vinylidene fluoride binder (PVDF, 15 wt%). The slurry cathode mixture was pasted on an Al foil and dried in vacuum oven. The cathode and anode electrodes were separated by Celgard 2400 membranes. The electrolyte was a 1 mol L^{-1} lithium hexafluorophosphate (LiPF_6) solution dissolved in ethylene carbonate (EC) and dimethyl carbonate (DMC) (EC:DMC = 1:1, by v/v ratio). Galvanostatic charge–discharge cycling was performed on a Land® (Wuhan, China) battery tester. Electrochemical impedance spectroscopy was collected on a ZAHNER®-IM6e electrochemical workstation. The impedance spectra were recorded by applying an ac voltage of 5 mV in the frequency range from 1 MHz to 1 mHz.

3. Results and discussion

Fig. 1 shows the X-ray diffraction patterns of the LVP and LVP-Cu samples, together with the vertical lines those stand for the typical diffractions of Cu metal (PDF#03-1005) as a reference. It is seen from the figure that both the characteristic peaks of Cu (1 1 1) and (2 0 0) could be detected in the LVP-Cu composite. But the peaks are very weak due of the small amount of copper. Except for the diffractions of copper, all of the peaks could be indexed to the monoclinic $\text{Li}_3\text{V}_2(\text{PO}_4)_3$ structure with space group of $P2_1/n$. Since the radius of copper cations (0.91 and 0.86 Å for Cu^+ and Cu^{2+} , respectively) are much bigger than that of V^{3+} (0.74 Å), if Cu was doped in the lattice of $\text{Li}_3\text{V}_2(\text{PO}_4)_3$, it would lead to an increase in the lattice parameters of the sample. For this reason, the lattice parameters of the samples were calculated from the XRD results. The (a , b , c , β) parameters of LVP-Cu are (8.608 Å, 8.593 Å, 12.047 Å, 90.2°), which are in concordant with those of LVP, i.e. (8.607 Å, 8.595 Å, 12.046 Å, 90.1°). This suggests that Cu did not enter the crystal structure of $\text{Li}_3\text{V}_2(\text{PO}_4)_3$ and the $\text{Li}_3\text{V}_2(\text{PO}_4)_3/\text{Cu}$ composite was a mixture of Cu metal and $\text{Li}_3\text{V}_2(\text{PO}_4)_3$. The mean coherent domain size of the materials were calculated by the Scherer formula, which are 37 nm and 47 nm for $\text{Li}_3\text{V}_2(\text{PO}_4)_3$ and $\text{Li}_3\text{V}_2(\text{PO}_4)_3/\text{Cu}$, respectively.

Fig. 2 shows the SEM images of the samples. It is seen that both the LVP and LVP-Cu particles are in micrometer scale. But the particle size of LVP-Cu is a little bit bigger than that of LVP. Under a higher

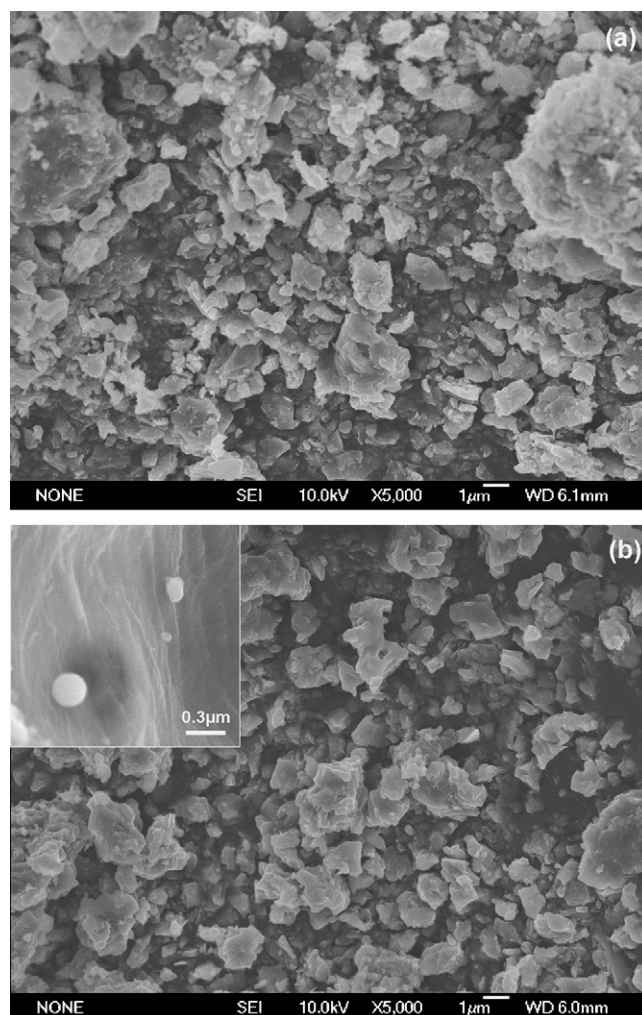


Fig. 2. SEM images of the LVP (a) and LVP-Cu (b) samples.

magnification (insert of **Fig. 2b**), some white-colored small particles can be observed on the particle surface of LVP-Cu. Energy dispersive spectroscopy (**Fig. 3**) confirms that they are the Cu particles in the composite.

The electronic conductivity of LVP was measured to be $1.1 \times 10^{-4} \text{ S cm}^{-1}$, which is much higher than that of pristine $\text{Li}_3\text{V}_2(\text{PO}_4)_3$, i.e. $9 \times 10^{-8} \text{ S cm}^{-1}$ [20]. This is due to the residual

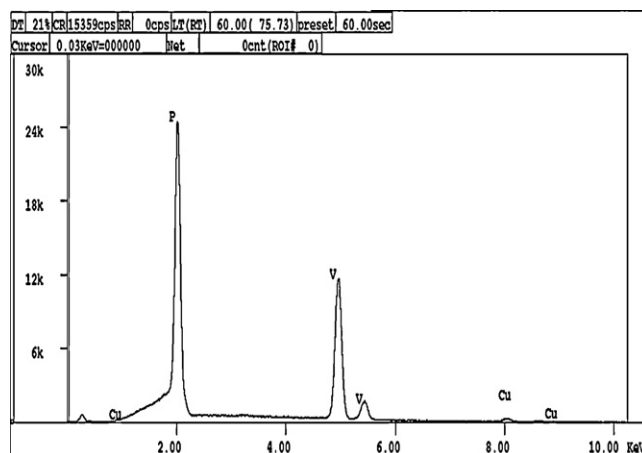


Fig. 3. Energy dispersive spectroscopy of the LVP-Cu sample.

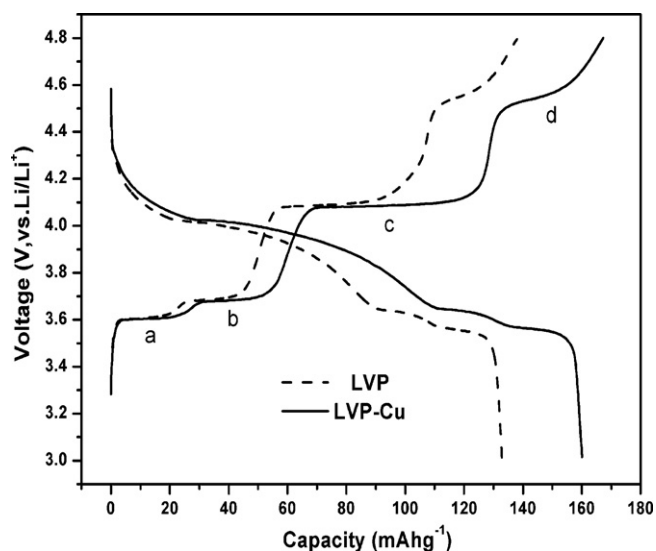


Fig. 4. First charge–discharge potential profiles of the LVP and LVP-Cu samples in the potential window of 3.0–4.8 V.

carbon in the material, which is usually found in $\text{Li}_3\text{V}_2(\text{PO}_4)_3$ when they are prepared using organic reduction species (such as sucrose) as raw materials [11,12,21]. The electronic conductivity of LVP-Cu is $2.5 \times 10^{-4} \text{ S cm}^{-1}$. It is seen that even Cu is an excellent electronic conductor, the electronic conductivity of LVP-Cu was not prominently increased by adding of Cu. This is probably due to the fact that only a small amount of Cu was added. These Cu particles were not intimately dispersed on the material particles as shown in Fig. 2b.

Fig. 4 shows the first charge–discharge potential profiles of the materials in the potential window of 3.0–4.8 V. Both samples exhibit four charge plateaus, namely “a”, “b”, “c” and “d”. These plateaus correspond to the two-phase transitions between the single phases of $\text{Li}_x\text{V}_2(\text{PO}_4)_3$ ($x=2.5, 2.0, 1.0$ and 0). The LVP-Cu composite has an initial discharge capacity of 160 mAh g^{-1} , which is much higher than that of LVP (132 mAh g^{-1}). This shows that the LVP-Cu composite has faster electrochemical kinetics with respect to that of LVP. Fig. 5 displays the cycling performance of the samples at $C/10$ rate. It is clear to see that the LVP-Cu composite exhibits higher discharge capacities than LVP. The discharge capacity of

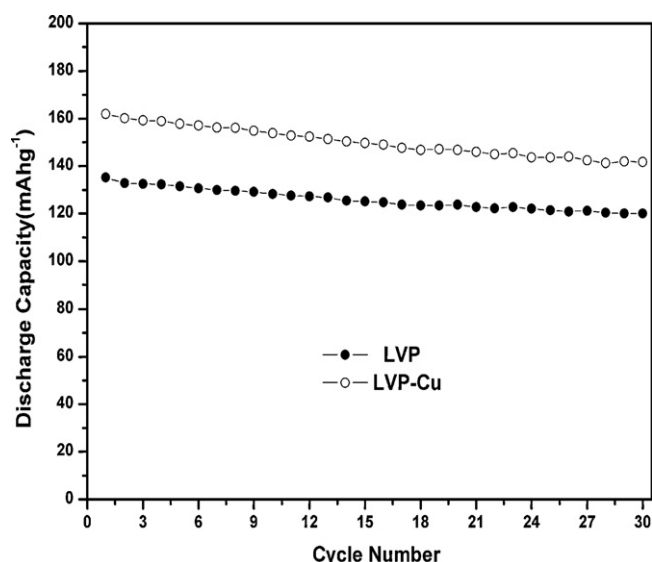


Fig. 5. Cycling performance of the LVP and LVP-Cu samples at $C/10$ rate.

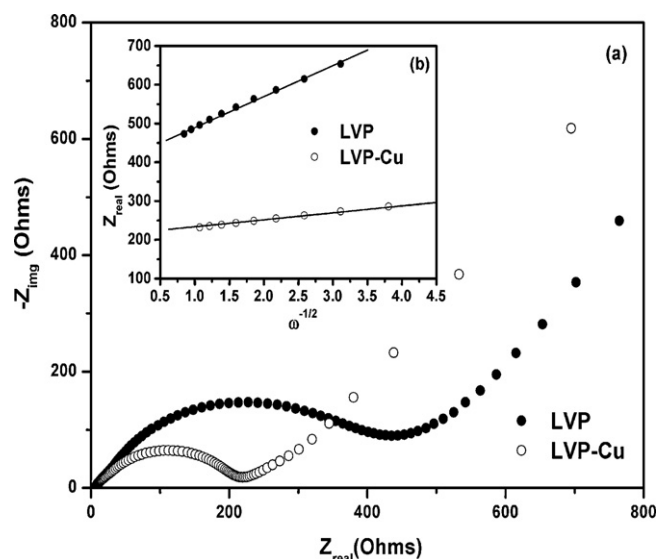


Fig. 6. (a) Nyquist plots of the LVP and LVP-Cu samples. (b) Linear fitting of the Z_{real} vs. $\omega^{-1/2}$ relationship.

LVP-Cu after 30 cycles is 141 mAh g^{-1} , which is much higher than that of LVP, i.e. 120 mAh g^{-1} .

Electrochemical impedance spectroscopy was carried out to study the electrochemical kinetics of the materials. Fig. 6a displays the Nyquist plots of the materials after charging and stabilizing the electrode at 4.0 V. The Nyquist plot is composed of a small intercept at high frequency, a semi-circle in the high to medium frequency region and a sloping line in the low frequency region. The small intercept is almost the same (6Ω) for both samples, which corresponds to the internal resistance (R_s) of the battery. The semi-circle corresponds to the charge transfer resistance (R_{ct}) and double layer capacitance. The sloping line corresponds to the diffusion of Li^+ in the electrode bulk, namely the Warburg impedance. The charge transfer resistance of LVP-Cu is 198Ω , which is much smaller than that of LVP, i.e. 492Ω . The lithium diffusion coefficient of the materials, D_{Li} , could be calculated from the Warburg region using the following equation [22,23]:

$$D_{\text{Li}} = \frac{0.5R^2T^2}{S^2n^4F^4C^2\sigma^2} \quad (1)$$

where R is the gas constant, T the absolute temperature, S the surface area of the electrode, n the number of electrons involved in electrochemical reaction, F the Faraday constant, and σ the Warburg factor which obeys the following relationship,

$$Z_{real} = R_s + R_{ct} + \sigma\omega^{-1/2} \quad (2)$$

The slope σ can be obtained based on a linear fitting of Z_{real} vs. $\omega^{-1/2}$ as shown in Fig. 6b. Using the value of σ and Eq. (1) the lithium diffusion coefficient of LVP is calculated to be $1.3 \times 10^{-9} \text{ cm}^2 \text{ s}^{-1}$, which fit well with the previous report [24]. The lithium diffusion coefficient of LVP-Cu is enhanced by 20 times to $2.8 \times 10^{-8} \text{ cm}^2 \text{ s}^{-1}$ by Cu adding.

The lithium diffusion coefficient can be expressed as a product of a self-diffusion coefficient $D_{\text{Li}(self)}$ and a thermodynamic or Wagner factor Φ [25]:

$$D_{\text{Li}} = D_{\text{Li}(self)} + \Phi \quad (3)$$

$D_{\text{Li}(self)}$ and Φ are very sensitive to the structural and electrical properties of an intercalation material, respectively [26]. X-ray diffraction showed that the structure of $\text{Li}_3\text{V}_2(\text{PO}_4)_3$ was not changed by Cu addition. Therefore, the larger lithium diffusion coefficient of LVP-Cu should be related with its higher electronic

conductivity. The Wagner factor, Φ , depends on the mobility and concentration of ions and electrons in the active material. During electrochemical reaction, electrons move ahead of Li^+ ions and generate an internal electrical field in which the ions diffusion is accelerated. Thus, fundamentally a higher electronic conductivity can cause a faster Li^+ diffusion. This explains why the lithium diffusion coefficient of $\text{Li}_3\text{V}_2(\text{PO}_4)_3$ is improved by Cu addition.

4. Conclusions

We developed a simple method to prepare $\text{Li}_3\text{V}_2(\text{PO}_4)_3/\text{Cu}$ composite cathode materials. The Cu addition did not affect the crystal structure of $\text{Li}_3\text{V}_2(\text{PO}_4)_3$. There was only a slight increase in the electronic conductivity due to the small amount of Cu in the $\text{Li}_3\text{V}_2(\text{PO}_4)_3/\text{Cu}$ composite. However, the electrochemical kinetics was significantly improved, which was benefited from the larger electronic conductivity of the $\text{Li}_3\text{V}_2(\text{PO}_4)_3/\text{Cu}$ composite. These advantages led to the good cycling performance of the composite material.

Acknowledgements

This work was supported by MOST (No. 2009CB220104), NSFC (No. 50702024) and Graduate Innovation Fund of Jilin University (No. 20080103). The authors thank the Program for Changjiang Scholar and Innovative Research Team in University (No. IRT0625) and the Program for New Century Excellent Talents for financial supporting.

References

- [1] A.K. Padhi, K.S. Najundaswamy, J.B. Goodenough, J. Electrochem. Soc. 144 (1997) 1188.
- [2] X.F. Ouyang, M. Lei, S.Q. Shi, C.L. Luo, D.S. Liu, D.Y. Jiang, Z.Q. Ye, M.S. Lei, J. Alloys Compd. 476 (2009) 462.
- [3] A.Y. Shenouda, H.K. Liu, J. Alloys Compd. 477 (2009) 498.
- [4] S. Okada, S. Sawa, M. Egashira, J.I. Yamaki, M. Tabuchi, H. Kageyama, T. Konishi, A. Yoshino, J. Power Sources 97 (2001) 430.
- [5] C. Delacourt, P. Poizot, M. Morcrette, J.M. Tarascon, C. Masquelier, Chem. Mater. 16 (2004) 93.
- [6] H. Huang, S.C. Yin, T. Kerr, N. Taylor, L.F. Nazar, Adv. Mater. 14 (2002) 1525.
- [7] S.C. Yin, H. Grondley, P. Strobel, M. Anne, L.F. Nazar, J. Am. Chem. Soc. 125 (2003) 10402.
- [8] J. Gaubicher, C. Wurm, G. Goward, C. Masquelier, L. Nazar, Chem. Mater. 12 (2000) 3240.
- [9] S.Q. Liu, S.C. Li, K.L. Huang, B.L. Gong, G. Zhang, J. Alloys Compd. 450 (2008) 499.
- [10] C. Masquelier, A.K. Padhi, K.S. Nanjundaswamy, J.B. Goodenough, J. Solid State Chem. 135 (1998) 228.
- [11] Y.Z. Li, Z. Zhou, M.M. Ren, X.P. Gao, J. Yan, Electrochim. Acta 51 (2006) 6498.
- [12] M.M. Ren, Z. Zhou, X.P. Gao, W.X. Peng, J.P. Wei, J. Phys. Chem. C 112 (2008) 5689.
- [13] M.M. Ren, Z. Zhou, Y.Z. Li, X.P. Gao, J. Yan, J. Power Sources 162 (2006) 1357.
- [14] Y.H. Chen, Y.M. Zhao, X.N. An, J.M. Liu, Y.Z. Dong, L. Chen, Electrochim. Acta 54 (2009) 5844.
- [15] S.K. Zhong, L.T. Liu, J.Q. Liu, J. Wang, J.W. Yang, Solid State Commun. (2009), doi:10.1016/j.ssc.2009.06.019.
- [16] F. Croce, A.D. Epifanio, J. Hassoun, A. Deptula, T. Olczac, B. Scrosati, Electrochem. Solid State Lett. 5 (2002) A47.
- [17] S.H. Huang, Z.Y. Wen, X.L. Yang, Z.H. Gu, X.H. Xu, J. Power Sources 148 (2005) 72.
- [18] J.T. Son, K.S. Park, H.G. Kim, H.T. Chung, J. Power Sources 126 (2004) 182.
- [19] R. Guo, P. Shi, X. Cheng, Y. Ma, Z. Tan, J. Power Sources 189 (2009) 2.
- [20] S.C. Yin, P.S. Strobel, H. Grondley, L.F. Nazar, Chem. Mater. 16 (2004) 1456.
- [21] T. Jiang, C.Z. Wang, G. Chen, H. Chen, Y.J. Wei, X. Li, Solid State Ionics 180 (2009) 708.
- [22] X.Z. Liao, Z.F. Ma, Q. Gong, Y.S. He, L. Pei, L.J. Zeng, Electrochem. Commun. 10 (2008) 691.
- [23] T. Jiang, G. Chen, A. Li, C.Z. Wang, Y.J. Wei, J. Alloys Compd. 478 (2009) 604.
- [24] A. Tang, X. Wang, G. Xu, Z. Zhou, H. Nie, Mater. Lett. 63 (2009) 1439.
- [25] C. Wagner, J. Chem. Phys. 21 (1953) 1819.
- [26] L.A. Montoro, J.M. Rosolen, Electrochim. Acta 49 (2004) 3243.